4

Coastal landscape evolution

INTRODUCTION

Large seismic disturbances on the sea floor, submarine slides, and asteroid impacts with the ocean can create tsunami waves that spread ocean-wide with profound effects on coastal landscapes. They can generate run-up heights 30 times greater than their open ocean wave height and sweep several kilometers inland. This penetration inland can only be duplicated on flat coastlines by storms if they are accompanied by a significant storm surge. Tsunami are thus catastrophic events and can leave a permanent imprint on the landscape. There has been little appreciation in the literature that coastal landscapes may reflect tsunami processes rather than those induced by wind-generated waves and wind. Catastrophic events—termed catastrophism—are not well respected in modern science. This chapter will describe the role of catastrophism in the development of modern geological thinking, show in more detail how tsunami are different from storms, describe various models of tsunami-generated landscapes (Figure 4.1), and illustrate these models with examples from around the world.

CATASTROPHISM VS. UNIFORMITARIANISM

(Clifton, 1988; Alvarez, 1997; Bryant, 2005)

A tsunami was involved in one of the pivotal debates of modern scientific development. On November 1, 1755, an earthquake, with a possible surface wave magnitude, M_s, of 9.0, destroyed Lisbon, then a major center of European civilization. Shortly after the earthquake a tsunami swept into the city, and over the next few days fire consumed what was left of Lisbon. The event sent shock waves through the salons of Europe at the beginning of the Enlightenment. The earthquake struck on All Saints' Day, when many Christian believers were praying in church. John Wesley viewed the

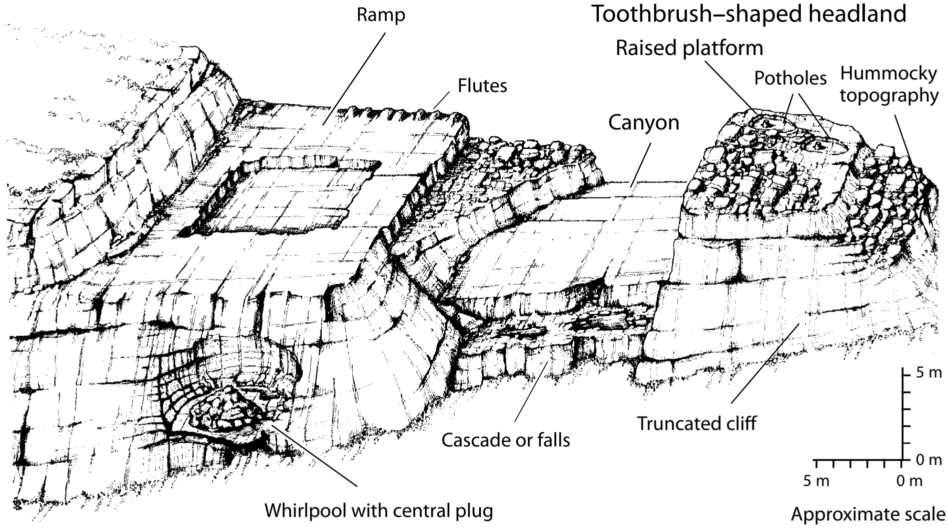

Figure 4.1. Model for irregular, large-scale, sculptured landscapes carved by tsunami. Model is for headlands 720 m above sea level. From Bryant and Young (1996).

Lisbon earthquake as God's punishment for the licentious behavior of believers in Lisbon, and retribution for the severity of the Portuguese Inquisition. Immanuel Kant and Jean-Jacques Rousseau viewed the disaster as a natural event and emphasized the need to avoid building in hazardous places. The Lisbon earthquake also gave birth to scientific study of geological events. In 1760, John Mitchell, geology professor at Cambridge University, documented the spatial effects of the earthquake on lake levels throughout Europe. He found seiching along the coastline of the North Sea and in Norwegian fjords, Scottish lochs, Swiss Alpine lakes, and rivers and canals in western Germany and the Netherlands. He deduced that there must have been a progressive, wave-like tilting of the Earth outward from the center of the earthquake and that this was different from the type of wave produced by a volcanic explosion.

Mitchell's work in 1760 on the Lisbon earthquake effectively represented the separation of two completely different philosophies for viewing the physical behavior of the natural world. Beforehand, the catastrophists—people who believed that the shape of the Earth's surface, the stratigraphic breaks evidenced in rock columns, and the large events that were associated with observable processes were cataclysmic—dominated geological methodology. More important, these catastrophic processes were Acts of God. The events had to be cataclysmic in order to fit the many observable sequences observed in the rock record into an age for the Earth of 4004 BC, determined from Biblical genealogy. Charles Lyell, one of the fathers of geology, sought to replace this catastrophe theory with gradualism—the idea that geological and geomorphic features were the result of cumulative slow change by natural processes operating at relatively constant rates. This idea implied that processes that shape the Earth's surface followed laws of nature defined by physicists and mathematicians. Whewell, in a review of Lyell's work, coined the term *uniformitarianism*, and subsequently a protracted debate broke out on whether or not the slow processes we observe at present apply to past unobservable events. To add to the debate, the phrase "The present is the key to the past" was also coined.

In fact, the idea of uniformitarianism involves two concepts. The first implies that geological processes follow natural laws applicable to science. There are no Acts of God. This type of uniformitarianism was established to counter the arguments raised by the catastrophists. The second concept implies constancy of rates of change or material condition through time. This concept is nothing more than inductive reasoning: the type and rate of processes operating today characterize those that have operated over geological time. For example, waves break upon a beach today in the same manner as they would have a hundred million years ago, and prehistoric tsunami behave the same as modern ones described in our written records. If one wants to understand the sedimentary deposits of an ancient tidal estuary, one has to do no more than go to a modern estuary and study the processes at work. Included in this concept is the belief that physical landscapes such as modern floodplains and coastlines evolve slowly.

Few geomorphologists or geologists who study Earth surface processes and the evolution of modern landscapes would initially object to this concept. However, the concept does not withstand scrutiny. For example, there is no modern analogy to the nappe mountain building processes that formed the Alps, or to the mass extinctions and sudden discontinuities that have dominated the geological record. Additionally, no one who has witnessed a fault line being thrust up during an earthquake or Mt. St. Helens wrenching itself apart in a cataclysmic eruption would agree that all landscapes develop slowly. As Thomas Huxley so aptly worded it, gradualists had saddled themselves with the tenet of *Natura non facit saltum*—Nature does not make sudden jumps. J. Harlen Bretz from the University of Chicago challenged this tenet in the 1920s. Bretz attributed the formation of the scablands of eastern Washington to catastrophic floods. He subsequently bore the ridicule and rancor of the geological establishment for the next 40 years for proposing this radical idea. Not until the 1960s was Bretz proved correct when Vic Baker of the University of Arizona interpreted spaceprobe images of enormous channels on Mars as features similar to the Washington scablands. At the age of 83, Bretz finally received the recognition of his peers for his seminal work.

Convulsive events are important geological processes, and major tsunami can be defined as convulsive. More importantly, it will be shown in the remainder of this book that mega-tsunami—in many cases bigger than tsunami described in historic and scientific documents—have acted to shape coastlines. Some of these mega-tsunami events have occurred during the last millennium. In coastal geomorphology, existing scientific custom dictates that in the absence of convincing proof, the evidence for convulsive events must be explained by commoner events of lesser magnitude—such as storms. However, this restriction should not imply that storms could be ubiquitously invoked to account for all sediment deposits or coastal landscapes that, upon closer inspection, have anomalous attributes more correctly explained by a different and rarer convulsive process. The alternate phenomenon of tsunami certainly has the potential for moving sediment and molding coastal landscapes to the same degree as, if not more efficiently than, storms. Tsunami can also operate farther inland and at greater heights above sea level. Tsunami have for the most part been ignored in the geological and geomorphological literature as a major agent of coastal evolution. This neglect is unusual considering that tsunami are common, high-magnitude phenomena producing an on-surge with velocities up of $15\,m\,s^{-1}$ or more.

TSUNAMI VS. STORMS

(Coleman, 1968; Bourgeois and Leithold, 1984; Morton, 1988; Bryant, Young, and Price, 1996)

In the past, rapid coastal change, especially in sandy sediments, has been explained by invoking storms. Where sediments have previously incorporated boulders, the role of storms vs. tsunami has become problematic. However, much of the latter debate deals with isolated boulders or boulders chaotically mixed with sand deposited on low-lying coastal plains or atolls. The pattern of stacked and aligned boulders found along the New South Wales coast mainly lie above the limits of storm waves or surges. Where such boulders lie within the storm zone, they form bedforms that have never been linked to such events. More importantly, even a casual reconnaissance of the New South Wales coastline will show that storms inadequately account for the bedrock-sculptured features dominating the rocky coast. The uniform alignment of such forms, often not structurally controlled, also rules out chemical weathering. Along this coast, the largest storms measured this century in 1974 and 1978 only generated deep-water waves of 10.2 m, while the maximum probable wave for the coast is only a few meters higher. The effectiveness of these wave heights cannot be exacerbated at shore by storm surges because the narrowness of the shelf and the nature of storms limit surges here to less than 1.5 m. In addition, storm wave periods rarely exceed 15 seconds and then for only very short durations. Waves bigger than this, but more importantly, of several minutes duration, are required to account for the sustained high-velocity flows required to sculpture highly resistant bedrock into the features described in the previous chapter. Tsunami appear to be the only mechanism capable of providing these conditions along the coast.

The forms deposited by tsunami at the coastline can be confused with storm wave–built features. However, the internal fabric of such deposits is different from that produced by storm waves. For example, ridges and mounds built above the high-tide line at Bass Point, New South Wales, contain a chaotic mixture of boulders, gravel, sand, and shell. The steep sides of these landforms are presently being combed down by storm waves. Both the form and fabric of such features bear no relationship to storm wave or swell wave deposits. Their closest analog is an ice push ridge; however, the New South Wales coast last came under the influence of sea ice during the Permian, 200 million years ago.

The effect of backwash in tsunami is rarely mentioned in the literature. Near the coast, such flow is generally channelized as the volume of overwash drains seaward through inlets and along defined drainage channels. More importantly, undertow whereby flow in the water column moves seaward along the seabed can occur out to the shelf edge in depths of 100 m–130 m of water. Continental shelf profiles may be a product of repetitive combing by tsunami-induced currents. If this undertow contains any sediment, then it behaves as a density current and powerful ebb currents of $2\,m\,s^{-1}$–$3\,m\,s^{-1}$ can sweep down the continental slope and along the abyssal plain under the passage of a tsunami wave. These currents can scour the seabed and deposit sand and gravels considerable distances from the shelf edge. Such flows may account for the presence of coarse, winnowed, lag deposits and 2 m to 3 m diameter boulders at the toe of the continental slope in water depths of 200 m–400 m. The above processes cannot be mimicked by storm waves.

The nature of tsunami vs. storm deposits

(Bourgeois and Leithold, 1984; Shiki and Yamazaki, 1996; Dawson, 1999; Kortekaas and Dawson, 2007; Morton, Gelfenbaum, and Jaffe, 2007)

Storms are mainly responsible for two types of deposits: beaches consisting of gravels, cobbles, and boulders, and overwash sand splays. Unless storm waves can overwash a beach, sand is generally moved shoreward only by fair-weather swell. Gravel and cobble beaches are characterized by shape and size sorting of particles. Larger disk-shaped particles tend to move to the top of the beach where they are deposited as a berm that may develop at the limit of storm wave run-up. Smaller spherical particles tend to accumulate at the base of the foreshore. This difference is due to the greater potential for suspension transport of disks in swash and the greater rollability of spheres back down the beach face under backwash. Where sand is available, it tends to be trapped between the larger particles or accumulate at the bottom of the beach.

While tsunami can also overwash coasts and transport coarse sediment, the internal fabric of the deposits is distinctly different from those deposited by storm waves. First, sandy tsunami deposits rarely exceed 25 cm thickness, while storm deposits tend to be thicker than this. Second, tsunami can deposit layers of sediment up to several kilometers inland from the coast, whereas storms appear to build up an asymmetric wedge of coarse-grained sediment or berm that rarely extends 50 m – 100 m inland. Third, tsunami deposits drape over the landscape, while storm deposits tend to fill in the depressions. Fourth, while storm and tsunami deposits contain sand originating from beaches or dunes, tsunami deposits can contain finer sediment not found in these environments. The presence of angular rip-up clasts of mud or mud layers is characteristic only of tsunami deposits. Mud is winnowed from storm deposits by repetitive backwash while mud clasts are rounded within short distances by repeated contact with the bed. Fifth, a tsunami deposit tends to be massive with little evidence of bedding while a storm deposit tends to be bedded. No sediment-size zonation exists in coarse-grained tsunami deposits. Layers of fining upward sediment may be present in sandy tsunami deposits; however, such layers may not be visually evident or related to the number of tsunami waves. In storm overwash deposits, such layers relate to individual waves and appear as beds. Sixth, tsunami deposits along rocky coasts can contain a significant fraction of broken, angular, and rounded pebbles. Breakage is produced by intense turbulence as the tsunami makes contact with rocky shores or rips up material from shore platforms. Storm deposits may contain some angular and broken pebbles, but the amounts are much less. Finally, tsunami deposits can contain unbroken shell and foraminifera because flow may be laminar and dominated by suspension. This hinders particle-to-particle contact or particle contact with the bed. Storm waves carry particles in traction. Contact between particles and the bed are frequent such that shell and foraminifera show signs of fracturing and abrasion.

Gravel and cobble storm-built beaches tend to be characteristic of eroding coasts, although there are exceptions. Thus, their preservation potential is poor. Coarse-grained tsunami beach deposits have a higher potential for preservation, if not in the longer geological record, then certainly at high sea-level stillstands over the last few million years on tectonically stable coasts. These sediments often are deposited above the limits of storms, and unless eroded by subsequently larger tsunami, will remain stranded above the active coastal zone on such coasts.

Movement of boulders

(Bascom, 1959; Young, Bryant, and Price, 1996; Nott, 1997; Komar 1998; Solomon and Forbes, 1999)

Tsunami and storm waves differ in the way that they transport bouldery material. The forces of storm waves and their ability to destroy stony breakwalls and move large boulders on rock platforms are well documented. Under exceptional circumstances waves greater than 16 m have been recorded in the North Atlantic. There is evidence of a single boulder being tossed 25 m above sea level on the island of Surtsey in Iceland by such waves. Waves with a force of $3\,t\,m^{-2}$ in the 1800s moved blocks weighing 800 and 2,600 tonnes into the harbor at Wick, Scotland. Active pebble beaches sit 30 m above sea level on cliffs along the west coast of Ireland. In Hawaii, Hurricane Iniki in 1991 transported isolated boulders about 0.5 m in diameter along the coast of Maui. There are many stories of pebbles and even cobbles being hurled against lighthouse windows situated on cliff tops. Probably one of the best-documented incidences showing the ability of storms to transport coarse material to the tops of cliffs occurred during Tropical Cyclone Ofa on the south coast of Niue in the southwest Pacific on February 5, 1990. Niue is a raised, relict coral atoll fringed by limestone cliffs rising up to 70 m above sea level. A platform reef, up to 120 m wide, has developed at the base of the cliffs. Ofa generated winds of more than $170\,km\,h^{-1}$ and waves with a maximum significant height of 8.1 m. As it approached Niue, it produced waves 18 m high along the coast. The effect of these waves along the cliffs was dramatic. At Alofi, waves broke above the roof of a hospital situated on an 18 m high cliff. The lower floor of a hotel was severely smashed by the impact of storm-tossed debris. Coarse gravel and boulders 2 m–3 m in diameter were flung inland over 100 m from the cliff line.

Isolated boulders tossed by storms, however, are different from the accumulations of boulders deposited by tsunami. The analysis used in the previous chapter to

Table 4.1. Comparison of tsunami and storm wave heights required to transport the boulders mentioned to this point in the text.

Location	*Boulder width* (m)	*Height of tsunami at shore* (m)	*Breaking storm-wave height* (m)
Jervis Bay			
Mermaids Inlet	2.3	1.4	5.6
Little Beecroft Head			
Ramp	4.1	2.7	10.8
Clifftop	1.1	0.7	2.8
Honeysuckle Point	2.8	1.8	7.2
Tuross Head	1.3	0.8	3.2
Bingie Bingie Point	2.8	1.8	7.2
O'Hara Headland	1.1	0.7	2.8
Sampson Point, WA	1.0	0.6	2.4
Flores, Indonesia	1.5	2.0	8.0

Source: Based on Young et al., 1996a.

define the wave height of tsunami capable of moving boulders of different shape and size can be applied to storm waves. The velocity of a wind-generated storm wave breaking at the shoreline can be approximated as follows:

$$v = (gH_b)^{0.5} \tag{4.1}$$

This is half the velocity of an equivalent tsunami wave at shore. When Equation (4.1) is combined with Equations (3.3)–(3.5) and solved for wave height, the following relationship is obtained:

$$H_b \geq 4H_t \tag{4.2}$$

This relationship holds for exposed and submerged boulders, and those that have originated from bedrock surfaces. Table 4.1 presents a comparison of the wave heights of tsunami and storms necessary to transport the boulders described so far in this book. Clearly, tsunami waves are more efficient than storm waves at transporting boulders inland. This fact becomes more relevant knowing that storm waves break in water depths 1.28 times their wave height. Hence, the heights for storm waves shown in Table 4.1 require much larger waves offshore to overcome the effects of wave breaking. Storm waves lose little energy only along coasts where cliffs plunge into the ocean. Unless storm waves reach a platform before breaking, they do not have the capability to move boulders more than 2 m in diameter on most rocky coasts. While storm waves under ideal conditions can transport boulders, as shown by the effect of Cyclone Ofa on the island of Niue, they are very unlikely to transport boulders and deposit them in imbricated piles at the top of cliffs. Boulder imbrication in contrast to pebble imbrication is rarely referenced in the coastal literature. Along the New South Wales south coast, imbrication is a dominant characteristic of boulder piles and a signature of tsunami. For example, at Tuross Heads, contact-imbricated boulders with an upstream dip of 30°–50° are piled *en echelon* in two single files over a distance of 150 m. This pattern is similar to that produced in erosive fluvial environments by high-magnitude, unidirectional flow. The size of the imbricated boulders not only matches that produced by high-magnitude flows in streams but also that produced by the catastrophic flows hypothesized for meltwaters in front of, or beneath, large glaciers. These imbricated piles do not require continuous flow, but rather a simple succession of three or more large waves—a feature that is commonly characteristic of a tsunami wave train.

TYPES OF COASTAL LANDSCAPES CREATED BY TSUNAMI

The modeling of spatial variation in modern sedimentary environments dominated by a specific process is termed a facies model. These models are well formulated for many processes such as tides, rivers, and waves. Facies models are used to interpret the geological rock record. Rarely do facies models consider bedrock erosion. For example, while much literature has been written on the formation of beaches with their attendant surf zones and the long-term development of sandy coastal barriers, little has been written on the erosion of rocky coasts by waves. What has been written is elementary and perfunctory. What is a sea cave, a coastal stack, or an arch? The literature frequently refers to such features but sheds little light as to their formation, especially in resistant and massively bedded bedrock. Even the formation of rock platforms, the most studied feature of rocky coasts, is ambiguous. Erosion of platforms across bedrock of differing lithologies or structures is attributed to long-term wave abrasion or chemical erosion—processes that have been measured at localized points but never broadly enough to establish them as the main processes. Catastrophic tsunami waves have the power to erode such surfaces in one instant. Many other aspects of cliffed and rocky coasts are treated in a similarly cursory fashion. If sea caves, stacks, arches, bedrock-ramped surfaces, sheared cliffs, imbricated boulder piles, and chevron ridges are the signature of tsunami, then how common are catastrophic tsunami in shaping the world's coastline?

Sandy barrier coasts

(Minoura and Nakaya, 1991; Andrade, 1992)

Large sections of the world's sandy coastline are characterized by barriers either welded to the coastline or separated from it by shallow lagoons. The origin of these barriers has been attributed to shoreward movement of sediment across the shelf by wind-generated waves, concomitantly with the Holocene rise of sea level. Lagoons form where the rate of migration of sand deposits lags the rate at which the rising sea drowns land. This theory of barrier formation ignores the role of tsunami as a

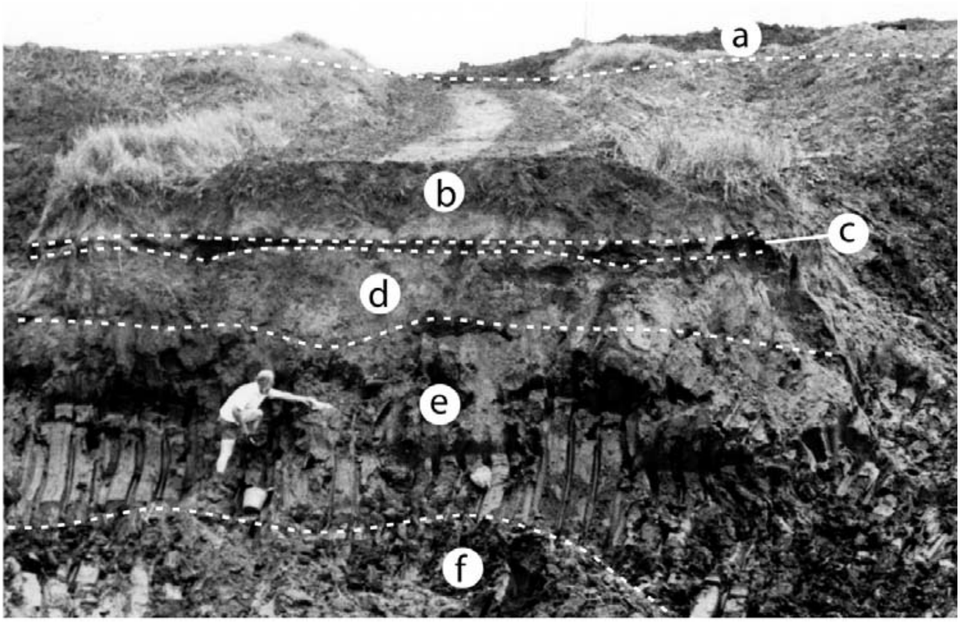

Figure 4.2. Section through the barrier beach at Bellambi, New South Wales, Australia: (a) modern dune, (b) Holocene barrier sand dated using thermoluminescence (TL) at 7400 BP, (c) clay unit, (d) tsunami sand TL-dated at 25,000 BP, (e) Holocene estuarine clay radiocarbon-dated at 5100 BP, and (f) Pleistocene estuarine clay TL-dated at more than 45,000 years in age. The TL date of the tsunami sand indicates that the sands are anomalous. The Holocene ages overlap.

possible mechanism, not only for shifting barriers landward, but also for building them up vertically. For example, at Bellambi along the New South Wales coast of Australia, tsunami-deposited sands make up 20% to 90% of the vertical accretion of a barrier beach that stands 3 m–4 m above present sea level (Figure 4.2). This beach will be described in more detail subsequently.

Tsunami in shallow water are constructional waves with the potential to carry large amounts of sand and coarse-grained sediment shoreward. Large eolian dunes that may develop on stable barriers do not necessarily impede tsunami. Instead, tsunami can overwash such forms, reducing the height of the dunes, depositing sediment in dune hollows, and spreading sand as a thin sheet across backing lagoons (Figure 4.3). On the other hand, storm waves tend to surge through low-lying gaps in dune fields, sporadically depositing lobate washover fans in lagoons. Rarely will these fans penetrate far into a lagoon or coalesce. The seaward part of the barrier can also be translated rapidly landward tens of meters by the passage of a tsunami. This occurred along the barrier fronting Sissano lagoon during the Papua New Guinea tsunami of July 17, 1998. The welding of a barrier to a coastline overtop lagoonal sediments may signify the presence of recent tsunami along a coast where historical evidence for such events is lacking. Pre-existing tidal inlets are preferred conduits for

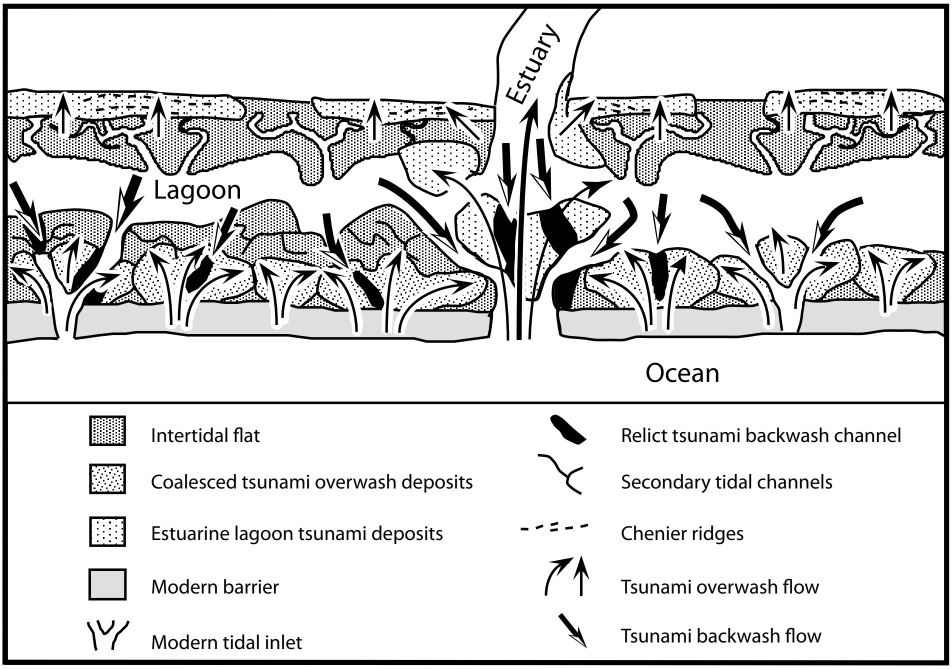

Figure 4.3. Model of the effect of tsunami upon a sandy barrier coastline. Based on Minoura and Nakaya (1991), and Andrade (1992).

tsunami. Sediment-laden tsunami may deposit large, coherent deltas at these locations, and these may be mistaken for flood tidal deltas. These features may be raised above present sea level or form shallow shoals inside inlets. Because the sediment was deposited rapidly, these deltas may end abruptly landward in lagoons and estuaries, forming sediment thresholds that are stable under present-day tidal flow regimes. Channels through the lagoon can also be scoured by tsunami, with sediment being deposited on the landward side of lagoons as splays.

If the volume of sand transported by a tsunami is large, then a raised backbarrier platform may form from coalescing overwash fans or smaller lagoons may be completely infilled. The height of either the backbarrier platform or infilled lagoon may lie several meters above existing sea level. These raised lagoons may be misinterpreted as evidence for a higher sea level. If these surfaces are not covered by seawater or quickly vegetated, they may be subject to wind deflation, with the formation of small hummocky dunes. Under extreme conditions, tsunami waves may cross a lagoon, overwash the landward shoreline, and deposit marine sediment as chenier ridges. Such ridges ring the landward sides of lagoons in New South Wales. Finally, along ria coastlines, estuaries may be infilled with marine sediment for considerable distances up-river. High-velocity flood and backwash flows under large tsunami may form pool and riffle topography. This process may account for pools that are tens of meters deep and morphologically stable under present tidal flow regimes in coastal estuaries along the New South Wales coast.

Water piled up behind barriers by tsunami overwash tends to drain seaward through existing channels. However, if the tsunami wave crest impinges at an angle to the coast, channels can be opened up, or widened, at the downdrift end of barriers. In some cases, on low barriers, water may simply drain back into the ocean as a sheet along the full length of the barrier. Because barriers are breached at so many locations, the resulting tidal inlets that form compete for the available tidal prism rushing into the lagoon under normal tides. As these inlets become less efficient in flushing out sediment, they lose their integrity and rapidly close. Hence, tsunami-swept barriers may show evidence of numerous relict tidal inlets without any obvious outlet to the sea. Reorganization of tidal flow in the lagoon because of these openings may lead to the formation of a secondary, shallow, bifurcating distributary channel network. In contrast, under storm waves, new tidal inlets are usually located opposite, or close to, contemporary estuary mouths.

Deltas and alluvial plains

(Young *et al.*, 1995, Young, White, and Price, 1996)

The pattern on deltas and alluvial plains is different. If these low-lying areas are cleared of vegetation, the low frictional coefficient permits the tsunami wave to penetrate far inland before its energy is dissipated. The limit of penetration is defined by Equation (2.14). In this instance, the wave can deposit silt or sand as a landward-tapering unit ranging from a few centimeters to over a meter in thickness. This feature is the most commonly identified signature of tsunami as described in Chapter 3. In some cases this sand unit can be deposited 10 km or more inland. In extreme cases, where sand is abundant, a swash bar or chevron ridge may be deposited at the landward limit of penetration. Very little attention has been paid to the resulting backwash, which according to hydrological principles must become concentrated into a network of interconnected channels that increase in size, but decrease in number, seaward. Only one description of such a network has appeared in the literature to date, and this is for the Shoalhaven Delta on the New South Wales south coast (Figure 3.3a). Here a large tsunami event deposited a fine sand unit up to 10 km from the coast. The sand contains open marine shells, such as *Polinices didymus*, *Austrocochlea constricta*, and *Bankivia fasciata* that are 4,730–5,050 years old.

A network of meandering backflow channels drains off the delta to the southeast (Figure 4.4). Significantly, these smaller channels are elevated above the regional landscape and are bordered by broad swamps. These channels are distinct from the main channel of the Shoalhaven River in that they have developed within Holocene sediment, whereas the river is entrenched into a Pleistocene surface that is buried about 4 m below the surface of the delta. The backwash channels are not only an order of magnitude smaller than the main river, but they also have a much lower carrying capacity. The channels increase in width from 40 m about 10 km upstream to

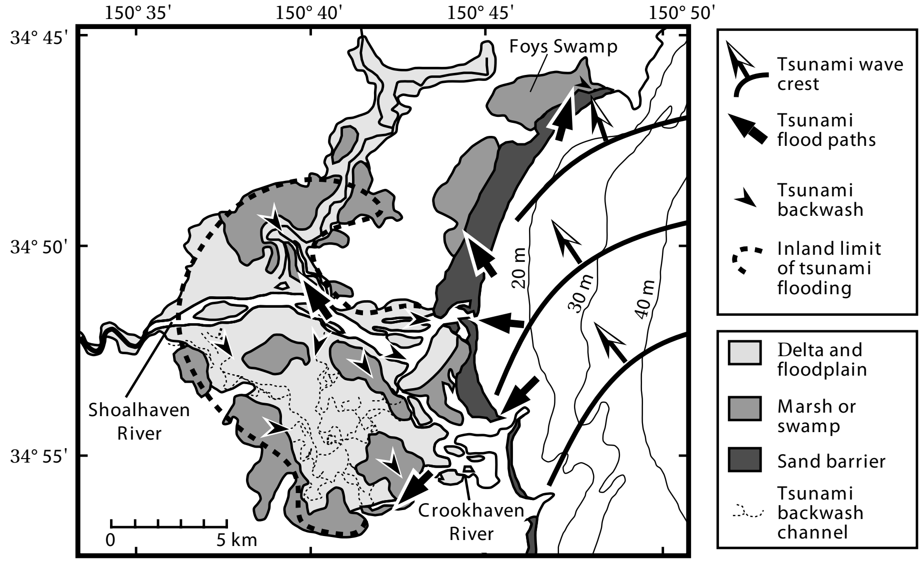

Figure 4.4. Hypothesized tsunami overwashing the Shoalhaven Delta, New South Wales, and the meandering backwash channels draining water off the Delta. A tsunami event 4,730–5,050 years ago—as determined from shell buried within a tapering sand layer within the Delta—probably created these channels. The extent of this marine layer is also marked. A younger tsunami event around AD 1410 ± 60 years may also be implicated in the formation of the backwash channels. Based on Young, White, and Price, (1996).

100 m at the mouth of the Crookhaven River, which exits to the sea at the sheltered southeast corner of the delta. The channels had a maximum discharge of 500 $m^3 s^{-1}$ based upon the length of meanders. The modern Shoalhaven River has a bankfull discharge of 3,000 $m^3 s^{-1}$ in flood. Many smaller streams were once tidal, but the channels have since undergone infilling with a reduction in their carrying capacity. The channels are 600 years old, coinciding with the regional age of a large paleo-tsunami predating European settlement. This age was obtained from oyster shells found on a raised pile of imbricated boulders that were swept into the entrance of the Crookhaven River as the tsunami approached from the south. The wave then climbed onto the delta via this entrance and the main channel of the Shoalhaven River (Figure 4.4). The inferred direction of approach coincides with the alignment of nearby boulders deposited by tsunami on cliffs rising 16 m–33 m above sea level (Figure 3.13). The tsunami also swept over a coastal sand barrier and onto the northern part of the delta (Foys Swamp), depositing a layer of sand and cobble 1.8 km inland of the modern shore. The small meandering channels on the southern part of the delta were created by southeast drainage of backwash from the deltaic surface after the tsunami's passage northward up the coast.

Rocky coasts

(Bryant and Young, 1996)

There are two distinct models of sculptured landscape for rocky coasts: smooth, small-scale and irregular, large-scale. These are shown schematically in Figures 4.5 and 4.1, respectively. The two models can be differentiated from each other by their degree of dissection. Smooth, small-scale bedrock-sculptured landscapes are restricted to headlands less than 7 m–8 m in height. Features consist of *S*-forms and bedrock polishing, and rarely exceed a meter in relief. Dump deposits and imbricated boulders usually are present nearby. The *S*-forms are directional, paralleling each other and the orientation of any imbricated boulders. The landscape is dominated on the side of headlands facing the tsunami by fields of overlapping muschelbrüche and sichelwannen grading into V-shaped grooves as slopes steepen. Where vertical vortices develop, broad potholes may form, but rarely with preserved central bedrock plugs. Crude transverse troughs develop wherever the slope levels off. At the crest of headlands, muschelbrüche-like forms give way to elongated fluting. The flutes taper downflow into undulating surfaces on the lee slope. Sinuous cavitation marks and drill holes develop on this gentler surface wherever flow accelerates because of steepening or flow impingement against the bed. On some surfaces, a zone of fluting and cavitation marks may reappear toward the bottom of the lee slope because of flow acceleration. Cavettos or drill holes develop wherever vertical faces are present. While cavettos are restricted to surfaces paralleling the flow, cavitation marks are ubiquitous.

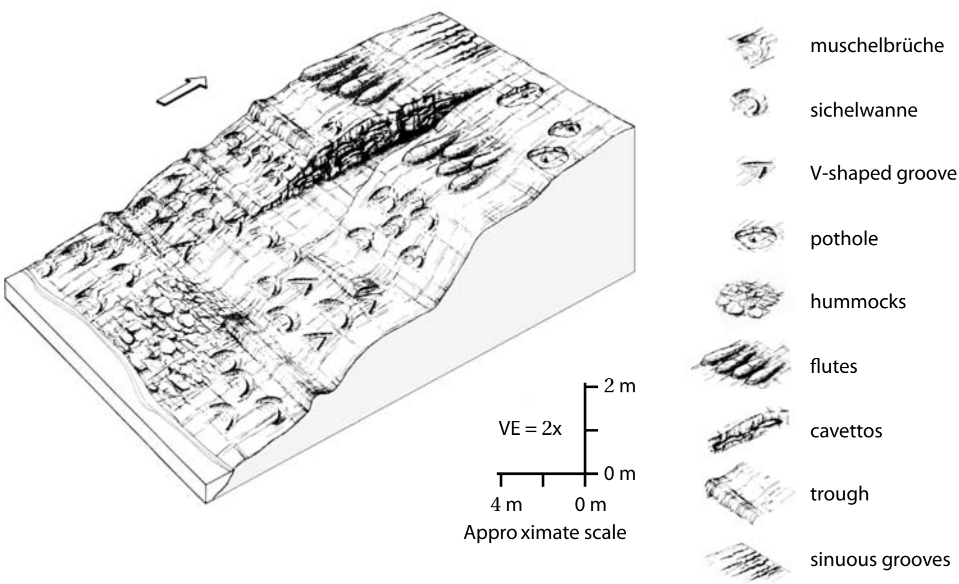

Figure 4.5. Model for smooth, small-scale, bedrock surfaces sculptured by tsunami. Model is for headlands within 7 m of sea level. From Bryant and Young (1996).

Irregular, large-scale, bedrock-sculptured landscapes are most likely created by large tsunami generated by submarine landslides and asteroid impacts with the ocean. The landscape typically forms on headlands rising above 7 m–8 m elevation in exposed positions (Figure 3.23). Many facets of the small-scale model can be found in this landscape. The large-scale model is characterized by ramps, whirlpools, and canyons, forming toothbrush-shaped headlands (Figure 4.1). Ramps can extend from modern sea level to heights of 30 m and can evince zones of evacuated bedrock depressions (Figure 3.22), cascades, and canyons (Figure 3.23). Whirlpools up to 10 m–15 m deep (Figure 3.26) are found primarily on the upflow side of the headlands, although they can also form on steep lee slopes. The base of whirlpools generally lies just above mean sea level, but some are drowned, with the central plugs forming stacks that are detached from the coastline. The base of whirlpools is controlled by the depth of large-scale vortex formation rather than by the level of the sea at the time of formation. Smaller potholes are also found in these environments. Generally, canyon features are inclined downflow. However, where the effects of more than one event can be identified, earlier canyons provide conduits across the headland for subsequent, concentrated erosive flow. Irregular, large-scale landscapes preserve a crude indication of the direction of tsunami approach, although the effects of wave refraction may complicate the pattern. Under extreme conditions, the complete coastal landscape can bear the imprint of catastrophic flow—headlands from 80 m to 130 m high may be overwashed with sheets of water carving channels as they drained off the downflow side, headlands rising over 40 m above sea level may have their seaward ends truncated, talus and jagged bedrock may be stripped from cliff faces, platforms may be planed smooth to heights 20 m above sea level, and whole promontories may be sculptured into a fluted or drumlin-like shape. Finally, coastal tsunami flow is usually repetitive during a single erosive event, which consists of pulses of unidirectional, high-velocity flow as individual waves making up a tsunami wave train surge over bedrock promontories. In these instances, erosive vortices last for no more than a few minutes and the erosive event is completely over within a few hours.

Atolls

(Bourrouilh-Le Jan and Talandier, 1985; Talandier and Bourrouilh-Le Jan, 1988; Scoffin, 1993; Kench *et al.*, 2007)

The islands of the South Pacific are exposed to both tropical cyclones and tsunami. One of the more notable features is the occurrence of alternating mounds and channels. Mounds called *motu*, consisting of sands and gravels derived from the beach and reef, separate the channels or *hoa* from each other (Figure 4.6). The *motu* are drumlin-shaped with tails of debris trailing off into the lagoon. In many respects, they could also be interpreted as molded dump deposits. *Motu–hoa* topography appears to be restricted to atolls in the South Pacific. Many descriptions of this topography consider them features of storm waves. However, storm waves from tropical cyclones appear to modify prior *motu–hoa* topography rather than being responsible for it. Even under storm surge, bores generated by storms tend to flow

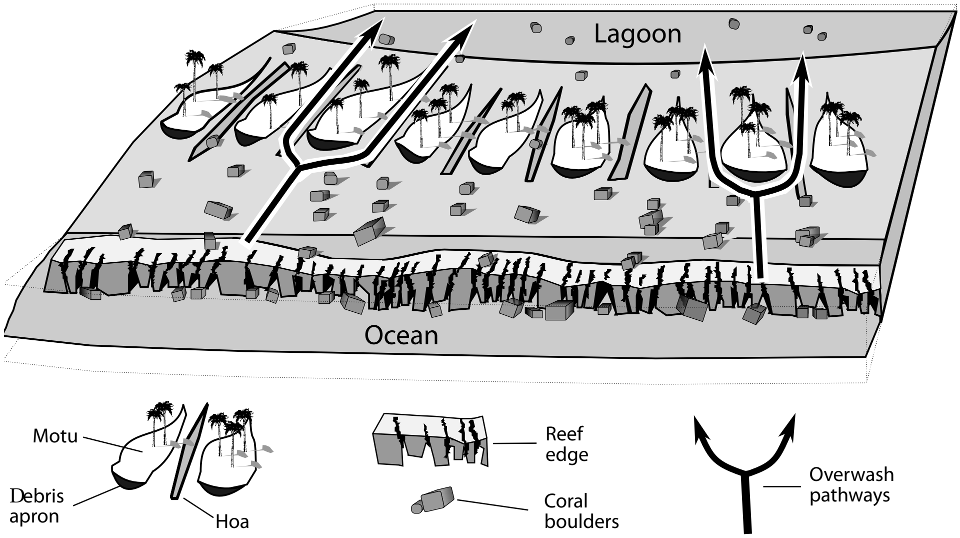

Figure 4.6. Model for the impact of tsunami upon coral atolls in the South Pacific Ocean. Based on Bourrouilh-Le Jan and Talandier (1985). Only a selection of overwash pathways around mounds (*motu*) and through channels (*hoa*) cutting across the atoll are marked.

through pre-existing *hoa* into the lagoon. Despite the steepness of nearshore topography around atolls, storm waves dissipate much of their energy by breaking on coral aprons fringing islands. The effect of storms is primarily restricted to the accumulation of coarse debris aprons in front of *motu–hoa* topography. For example, Cyclone Bebe in 1972 built a ridge on Funafuti that was 19 km long, 30 km wide, and 4 m high. The volume of sediment thrown into this ridge occupied 1.4×10^6 m^3 and weighed 2.8×10^6 tonnes. The ridge ran continuously in front of *motu–hoa* topography around the atoll. More often, changes in the landscape produced by storms are patchy, whereas *motu* and *hoa* form a regular pattern over considerable distances on many atolls. *Motu–hoa* topography can be formed by a single tsunami overwashing low-lying atolls. *Motu* or mounds form under helical flow where opposing vortices meet, while *hoa* or channels are excavated where these vortices diverge. The prominent nature of such topography suggests that mega-tsunami may be responsible.

Large boulders deposited on atolls are also difficult to link to storm waves. They have been ripped off the reef edge and deposited in trains or dumped in piles on the reef-fronting *motu*. In some cases, isolated boulders have been carried through *hoa* and deposited in the backing lagoon (Figure 4.6). This process has not been observed during storms. While storm waves can erode boulders from the reef edge, they rarely transport them far. In fact, boulders wrenched from the reef edge by storms usually end up in a wedge-shaped apron of talus at the foot of the reef slope. More unusual is the sheer size of some of the boulders. One of the best examples occurs on the northwest corner of Rangiroa Island in the Tuamotu Archipelago. Here, one of the coral boulders measures 15 m × 10 m × 5 m and weighs over 1,400 tonnes. This boulder could have been moved easily by a tsunami wave 6 m high—Equation (3.7)—but would have required a storm wave 24 m in height—Equation (4.2). Most boulders found scattered across atolls consist of coral that is more than 1,500 years old. However, the boulders rest on an atoll foundation that is as young as 300 years. This fact suggests that the boulders were deposited by a large tsunami at the beginning of the 18th century. Local legends in the South Pacific describe the occurrence of large catastrophic waves at this time concomitant with the abandonment of many islands throughout French Polynesia. Significantly, the legends have the Sun shining at the time of the waves—a fact ruling out tropical cyclones.

The Indian Ocean tsunami event of December 26, 2004 provided one of the few opportunities to observe the impact of a large tsunami upon atolls. This event will be described in detail in Chapter 5. On the Maldives, in the centerof the Indian Ocean, the first wave was 2.5 m high and surged over every atoll. This was followed over the next six hours by a succession of four to five diminishing waves at 15 min–140 min intervals. The waves eroded less than 4% of the islands; however, they played a major role in the redistribution of sediment that normally would have been produced by the accumulative effects of seasonal changes in wave climate. Sediment was removed from the eastern side of atolls fronting the tsunami and either draped as a layer of sand 10 cm–30 cm thick on top of the atoll or washed around the sides and deposited in the lee of islands. Where sediment was voluminous, this leeward deposition generated a trailing spit across the reef. Erosion at the front of the atoll left a permanent scarp that in many places exceeded 2 m in height. Nowhere did the waves erode channels or *hoa* across the atolls, a fact indicating that Pacific island *motu–hoa* topography must be produced by much higher energy events. Tsunami such as the Indian Ocean event are not detrimental to atolls, but rather a contributing factor in vertical island building.

EXAMPLES OF TSUNAMI-GENERATED LANDSCAPES: AUSTRALIA

(Young and Bryant, 1992; Bryant, Young, and Price, 1992, 1996; Young *et al.*, 1993, 1995; Young, Bryant, and Price, 1996; Young, White, and Price, 1996; Bryant *et al.*, 1997; Nott, 1997; Bryant and Nott, 2001; Nott and Bryant, 2003)

South coast of New South Wales

Many of the examples used as signatures of tsunami in Chapter 3 and in the construction of landscape models described in this chapter come from the south coast of New South Wales (Figure 3.3a). Dating evidence indicates that tsunami here have been a repetitive feature over the past 7,000 years. These tsunami have acted profoundly on the landscape at two scales. At the smaller scale, beaches have been overwashed, chaotically sorted sediments that include gravel and boulders have been dumped onto headlands, imbricated boulders have been deposited in aligned piles, and bedrock surfaces have been sculptured. At the larger scale, complete barrier sequences and rocky headlands bear the unmistakable signature of high-velocity flow that only tsunami can explain. While the evidence for tsunami as a dominant element of the landscape is pervasive, only a few examples can be presented in the space available here.

Many of the deltas and low coastal plains along this coast have been swept by tsunami. The model of tsunami overwash for deltas shown in Figure 4.4 is found here. Buried sand layers have also been identified in many estuarine settings. These units contain cobbles and marine shell, are up to 1 m thick, and can be found 10 km inland of the modern beach in sheltered positions that all but rule out deposition by normal wind-generated waves. Similar shell-rich sands have been found along the New South Wales coast trapped in sheltered embayments at Cullendulla Creek, Batemans Bay (Figure 3.8), and at Fingal Bay, Port Stephens. This coastline is also renowned for its sandy barriers entrapping large coastal lakes and enclosing lowlands. The evolution of these barriers has been explained in terms of high-frequency, low-magnitude marine and eolian processes superimposed on the effects of changing sea level during the Late Quaternary. The sandy barriers were constructed at sea level highstands during the Last Interglacial over 90,000 years ago, and during the Holocene between 3,000 and 7,000 years ago. Although sandy marine barrier deposits dating from the Last Interglacial are well preserved on the north coast of New South Wales, they are paradoxically rare south of Sydney, where many of the signatures of tsunami have been identified. Many of the Holocene barrier deposits are in fact the product of tsunami overwash.

Two examples stand out—Bellambi Beach, Wollongong, and the sand barriers inside Jervis Bay about 100 km south of Sydney (Figure 3.3a). At Bellambi, a 1.0 m to 1.2 m thick humate-impregnated sand that contains isolated, rounded boulders lies sandwiched between Holocene estuarine clay and beach sand (Figure 4.2). The humate is anomalous because the sand dates much older than the Holocene, at an age of 22,000 yr–25,600 yr. At this time, the coastline was nowhere near its present location, but 130 m lower and 12 km offshore. Significantly, a 20 cm to 30 cm thick pumice layer is trapped near the southern end of the barrier about 2 m above present sea level. The pumice is 25,000 years old and originated from volcanic eruptions north of New Zealand. Its composition does not match that of any modern pumice floating onto the coast. The pumice comes from relict beach deposits on the shelf. To maintain their older temporal signature, the humate sands were transported suddenly from the shelf to the present coastline during the building of the barrier. This process was carried out by a large tsunami about 4,500 yr–5,000 yr ago. The tsunami also picked up bouldery material from a headland 1 km away and mixed this with the sand. The pumice was not carried with any of this material. Being lighter than water, it floated to the surface of the ocean and drifted into the lagoon at the back of the barrier afterwards on sea breezes. If this scenario is correct, then the tsunami had to be large enough to generate bottom current velocities that could not only entrain sand, but also erode humate-cemented sediment from water depths of 100 m at the edge of the continental shelf. For this to happen, distinct from the capability of storm waves, the tsunami had to be over 5 m high when it reached the shelf edge.

Tsunami-deposited barriers in the Jervis Bay region consist of clean white sand that originated from the leached A2 horizon of podsolized dunes, formed at lower sea levels on the floor of the bay during the Last Glacial over 10,000 years ago. The barriers form raised platforms 1 km–2 km wide and 4 m–8 m above present sea level on a tectonically stable coast. The barriers supposedly were built up over the last 7,000 years; however, the sands yield an older age commensurate with their origin on the floor of the bay. Again, the sands must have been transported to the coast suddenly in order to maintain an older temporal signature. Transport occurred during one or more tsunami events.

The effect of tsunami on the rocky sections of this coast is even more dramatic. The scenic nature of many headlands is partially the consequence of intense tsunami erosion. Two headlands, Flagstaff Point and Kiama Headland, in the Wollongong area will be described here. Both headlands are similar in that they protrude seaward about 0.5 km beyond the trend of the coast. Both were affected by the same erosive tsunami traveling northward along the coast. The raised dump deposit and inverted keel-like stacks shown in the previous chapter are located between the two headlands (Figures 3.7 and 3.24, respectively). Flagstaff Point consists of massively jointed, horizontally bedded volcanic sandstones that have been deeply weathered, while Kiama Headland consists of weakly weathered, resistant basalt. Overwashing by high-velocity tsunami has severely eroded the seaward facets of both headlands, but with subtle differences. On Flagstaff Point, the tsunami eroded the softer material, forming a reef at the seaward tip and a rounded cliff along the southern side (Figure 4.7). The wave planed the top of the headland smooth, spreading a smear deposit that consists of muds, angular gravel, and quartz sand across this surface. The wave also moved massive boulders into imbricated piles on the eroded platform surface on the south side. However, the most dramatic features were created by tornadic vortices on the northern side of the headland. These vortices were 8 m – 20 m deep and rotated in a counterclockwise direction. The largest vortex was shed from the tip of the headland eroding a whirlpool with 20 m high sides into the cliff. Fluted bedrock on the outer surface of erosion outlines the vortex and its helical flow structure. The whirlpool is incomplete, indicating that the vortex developed toward the end of the wave's passage over the headland. As the wave wrapped around the headland, it broke as an enormous plunging breaker, scouring out a canyon structure along the northern side. The canyon is separated from the ocean by a buttress that rises 8 m above sea level at the most exposed corner, tapering downflow as the wave refracted around the headland. The tsunami then traveled across the sheltered bay behind the headland, carving giant cusps into a bedrock cliff on the other side. Finally, it swept inland depositing a large pebble- and cobble-laden sheet of sand up to 500 m inland.

At Kiama, the tsunami wave developed broad vortices, as water was concentrated against the southern cliff face (Figure 4.8). While flow probably obtained velocities similar to those at Flagstaff Point, the weakly weathered basalt was more resistant to erosion. Vortices eroded into the headland along major joints forming broad caves. At one location, a vortex penetrated 50 m–80 m along a joint, creating a cave that blew out at its landward end to form the Kiama Blowhole. Where the headland was lower in elevation, vortices began to scour out large muschelbrüche about 50 m in length. The tip of the headland, instead of being eroded into a reef, was

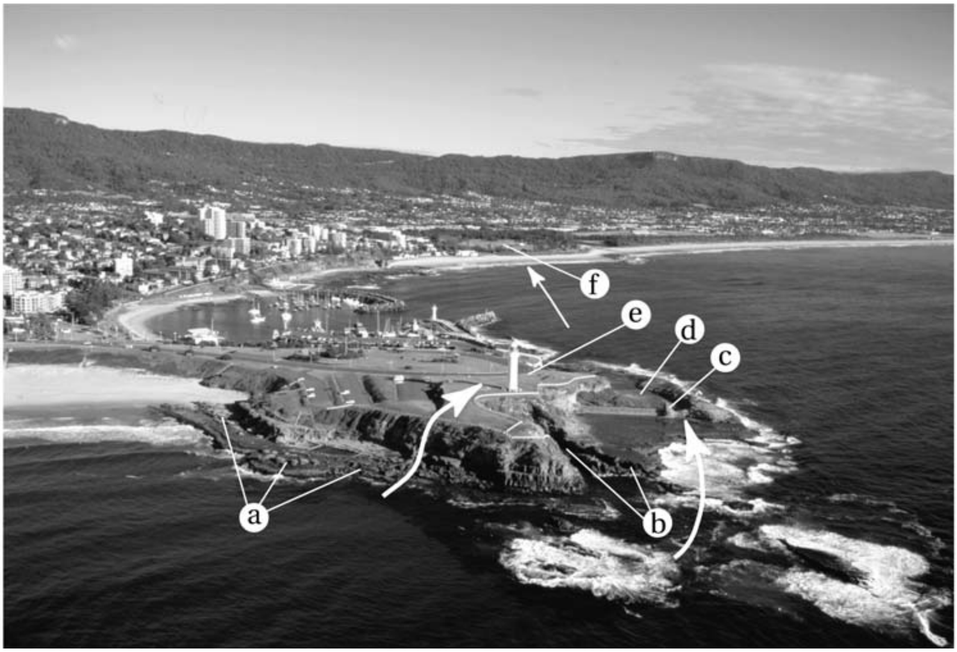

Figure 4.7. Flagstaff Point, Wollongong, Australia. This headland, which is 20 m above sea level, was overridden and severely eroded by a paleo-tsunami that approached from the southeast (white arrows). Main features (white lines) are as follows: (a) boulder piles, (b) incipient whirlpool with fluted rim, (c) plug, (d) canyon, and (e) smear deposit over headland. Sediment was transported across the bay and deposited as a sand sheet in the distance (f).

heavily scoured into hummocky bedrock topography to form a surface 8 m–10 m above sea level. Boulders were scattered across this surface. The wave also planed the top off the headland and deposited a 5 cm to 10 cm thick smear deposit that thickens downflow. The wave then crossed a small embayment in the lee of the headland, shearing the end off a cliff. Finally, the wave deposited quartz sand inland about a kilometer to the northwest.

Cairns coast, northeast Queensland

The signatures of tsunami are not restricted in Australia to the southeast coast. They also appear inside the Great Barrier Reef between Cairns and Cooktown along the northern Queensland coast (Figure 3.3b). This, at first, would appear to be unlikely. Even if tsunami have occurred in this part of the Coral Sea, the Great Barrier Reef should have protected the mainland coast. Evidence now suggests that tsunami have indeed reached the mainland coast with enough force, not only to transport boulders, but also to begin sculpturing bedrock. For example, at many locations, boulders weighing over a hundred tonnes can be found at elevations of 8 m–10 m above sea

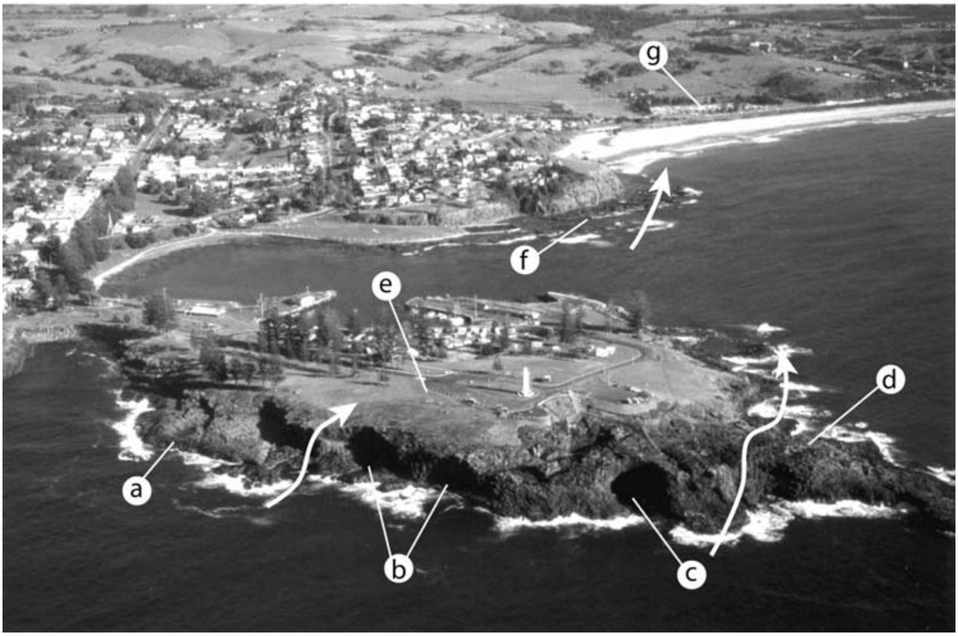

Figure 4.8. Kiama Headland lying 40 km south of Flagstaff Point (Figure 4.7). A paleo-tsunami also approached from the southeast (white arrows) and swept over the headland. Here caves have been bored into columnar basalts. Main features (white lines) are as follows: (a) large muschelbrüche-like feature, (b) incipient caves, (c) cave leading to blowhole, (d) hummocky topography on raised platform, (e) smear deposit over headland, and (f) sheared cliff face and planed platform. A sand sheet was again deposited across the bay (g).

level. One of the largest boulders is found at Cow Bay. It has a volume of 106 m^3 and weighs 286 tonnes. At Oak Beach, imbricated boulders weighing up to 156 tonnes and measuring over 8 m in length can be found in piles (Figure 4.9). Using Equations (3.4) and (4.2), it can be shown that tsunami rather than storm waves are the most feasible mechanism generating the flow velocities required to transport many of these boulders. These comparisons are presented in Table 4.2. All of the imbricated boulders can be transported by tsunami 5.0 m–11.2 m in height. The highest waves are required to move the boulders found at Cow Bay. The smallest storm wave must be 20 m high to move these boulders. This is virtually impossible because such a wave would break before reaching the coastline, even when superimposed on surges that can be up to 7 m high. The tsunami waves can generate theoretical flow velocities ranging from 3.7 $m\,s^{-1}$ to 10.4 $m\,s^{-1}$, with a mean value of 5.8 $m\,s^{-1}$. The highest of these velocities is more than sufficient to produce cavitation and sculpture bedrock. Indeed, many of the bedrock surfaces near the boulder piles evince bedrock-sculpturing signatures. For example, the boulders found at Oak Beach are emplaced on an undulatory, smooth surface characteristic of erosion by transverse roller vortices (Figure 4.9). *S*-forms are also evident on this bedrock surface.

Figure 4.9. Boulders stacked by tsunami on the platform at the south end of Oak Beach, North Queensland. The largest boulder is 4.0 m in diameter. Note the smoothed bedrock surface with evidence of large overlapping muschelbrüche.

Table 4.2. Comparison of tsunami and storm-wave heights required to transport boulders along the Queensland coast north of Cairns.

Location	*Boulder width* (m)	*Weight* (t)	*Height of tsunami at shore* (m)	*Breaking storm-wave height* (m)
Cow Bay	6.3	247.0	11.2	44.8
Oak Beach	4.0	192.0	5.0	20.0
Taylor Point	4.2	90.0	9.1	36.4
Turtle Creek Beach	4.3	115.0	5.2	20.8
Cape Tribulation	4.1	86.0	5.8	23.2

Source: Based on Nott (1997).

Figure 4.10. The eroded headland at the north end of Oak Beach, North Queensland. The flutes protruding above the raised platform surface face toward the south–southeast, the same direction as the alignment of boulders shown in Figure 4.9.

The northern headland of Oak Beach has also been dissected into a toothbrush shape that is covered with flutes, sinuous grooves, and cavitation drill holes (Figure 4.10).

The tsunami in the Cairns region have originated in the Coral Sea outside the Great Barrier Reef. It appears that probably paleo-tsunami penetrated the reef through openings such as Trinity Opening and Grafton Passage, which are more than 10 km wide and between 60 m and 70 m deep (Figure 3.3b). The alignment of boulders north of Cairns points directly toward Trinity Opening. At other locations, where the alignment of boulders is more alongshore, the tsunami waves appear to have been trapped through diffraction and refraction between the reef and the mainland, and by major headlands jutting from the coast at Cape Tribulation and Cairns.

Northwest West Australia

Signatures for both historical and paleo-tsunami exist along the coast of West Australia. The June 3, 1994 tsunami that originated in Indonesia swept the coast of the North West Cape through gaps in the Ningaloo Reef, resulting in the inland deposition of marine fauna, sand, and isolated coral boulders up to 2 m in width. Coral boulders were also swept through gaps in the coastal dunes and deposited 1 km inland across a flat, elevated plain by the tsunami following the eruption of Krakatau in 1883. Tropical cyclone storm surges have never reached this far inland on this coast. While some of the boulders were organized into piles, none shows any preferential alignment. These deposits can only be described as ephemeral dump deposits.

This contemporary evidence is dwarfed by the signature of paleo-tsunami along 1,000 km of coastline between Cape Leveque and North West Cape (Figure 3.3c). The magnitude of some of this evidence is the largest yet found in Australia. At Cape

Figure 4.11. Platform at Cape Leveque, West Australia. A paleo-tsunami swept over the island and cliffs in the background, and eroded the stack. Muschelbrüche outlined by the pools of standing water sculpture the platform surface. The bedrock surface was torn up along bedding planes. The boulders originated from the platform further seaward and were stacked in imbricated piles by flow traveling alongshore toward the camera.

Leveque, at least four waves from a paleo-tsunami dumped gravelly sands and shell in sheets and mounds along the coast, overriding headlands 60 m above sea level in some places. The sandstone platform in front of Cape Leveque was sculptured smoothly with the clear signature of large muschelbrüche, fluting, and transverse troughs. The seaward edge of this platform shows evidence of a preparation zone for boulders. Large slabs of bedrock 1 m–2 m thick were lifted repetitively up and down along bedding planes until they broke into blocks 4 m–5 m wide. At this point the fractured pieces were transported by tsunami flow and dumped alongshore into imbricated piles (Figure 4.11). A similar process is present at Broome. Here sands and gravels were dumped 5 km inland at the back of a flat headland. The angle of approach of waves at both locations appears to have been from the southwest—a direction not matching the modeled approach of tsunami from Indonesia. In the Great Sandy Desert, eolian ridges more than 30 km inland were truncated and remolded into chevron ridges by a paleo-tsunami. This distance is more than three times greater than the distance of penetration inland by any tsunami yet discovered for the south coast of New South Wales. Marine shell and lateritic gravels were deposited in these chevron dunes; lateritic boulders were stacked in front. Seven hundred kilometers farther south, at Exmouth on North West Cape, transverse dune ridges were overridden from the east by large waves. Coral, shell, and cobble were

Figure 4.12. Raised beds of cockles on a hill at Point Samson, northwest Western Australia. These shells extend 15 m above sea level. In this region, the paleo-tsunami flowed up the valley and over the hills in the background. The minimum age for the event, based on radiocarbon-dating of the shells, is AD 1080.

mixed with eolian sand and spread more than 2 km inland across the upper surface of at least seven dune ridges paralleling the coast.

By far the most dramatic evidence of tsunami occurs at Point Samson. Here, waves have impinged upon the coast from the Indian Ocean to the northeast. Shell deposits were laid down above the limits of storm surges (Figure 4.12) and on top of hills 15 m above sea level. In one extreme case, three layers of sand with a total thickness of 30 m were deposited in the lee of a hill over 60 m high and lying more than 500 meters inland. The sands contain boulder floaters, coral pieces, and shell. Each layer appears to represent an individual wave in a tsunami wave train. Dating of shell deposits in the region indicates that the tsunami occurred at the end of the 11th century, before European discovery. In a valley leading back from the coast, large mega-ripples with a wavelength approaching 1,000 m and consisting of cross-bedded gravels, have been deposited up to 5 km inland. The spacing between the mega-ripples is an order of magnitude greater than that found at Jervis Bay, New South Wales. The flow depth is theorized to have been as great as 20 m with velocities of over 13 m s^{-1}. The dip in the bedding indicates flow transport from the Indian Ocean. The gravels also contain boulders over 1 m in diameter that have been chiseled into a spherical shape (Figure 4.13). The tsunami waves overrode hills 60 m high, another 1 km inland, carving wind gaps 20 m deep through ridges. Sand and gravel were then

Figure 4.13. Chiseled boulders deposited in bedded gravels in a mega-ripple about 5 km inland of the coast at Point Samson, northwest Western Australia. The dip in bedding aligns with bedrock-sculptured features in the area (Figure 4.14) and shows flow from the northeast in the Indian Ocean.

deposited a further 2 km inland of these ridges. Finally, ridges 15 m high were sculptured into hull-shaped forms with bedrock plucked from the flanks and crest by helical flow that encompassed the whole height of the ridge (Figure 4.14). A cockscomb-like protuberance similar to that shown on the inverted keel-like stack in Figure 3.24 was eroded toward the front of the ridge by intense vortices or hydraulic hammering.

OTHER EXAMPLES OF TSUNAMI-GENERATED LANDSCAPES

Grand Cayman

(Jones and Hunter, 1992)

Other examples exist in the world where the signatures of tsunami dominate in preference to those induced by storms. The first of these examples comes from the

Figure 4.14. Streamlined inverted keel-shaped ridge with a cockscomb-like protuberance at Point Samson, northwest Western Australia. Note the resemblance of the cockscomb to that shown in Figure 3.22. The wave traveled from left to right. Intense vortices embedded in helical flow plucked blocks of bedrock from the sides of the ridge. The ridge is aligned with other bedrock features in the region. Scale is the person circled at the top.

Cayman Islands in the middle of the Caribbean Sea (Figure 4.15a). The island exists in a region where tsunami have played a major role in the region historically. For example, in June 1692, a powerful tsunami devastated Port Royal on the nearby island of Jamaica. The region is also dominated by tropical cyclones. For example, in 1785 a tropical cyclone destroyed every house and tree except one on the Cayman Islands. In 1932, a hurricane with winds of 330 km h^{-1} generated seas that carried huge rocks weighing several tonnes. The waves moved coral boulders 0.6 m–1.0 m in diameter shoreward from waters less than 15 m deep, constructing ramparts at shore.

Bigger boulders exist than those transported by these storms. The boulders appear to be related to a high-energy, historic event dating around 1662 that moved slabs as large as 5.5 m in length, depositing some in clusters up to 150 m inland. Some clusters contain imbricated stacks of boulders, aligned in a north–south direction, roughly at right angles to the shoreline. At Great Pedro Point, blocks weighing up to 10 tonnes were moved 18 m vertically and 50 m–60 m inland of the cliff line. The largest boulder measures 5.5 m $\times$ 2.8 m $\times$ 1.5 m. All of the boulders were emplaced at least 12 m above sea level. Many of the boulders originated as giant rip-up clasts torn from terraces formed in dolomite or from boulder deposits at the base of sea cliffs. The terraces had solutional weathering pinnacles and ridges with a relief of 2 m that were planed flat. According to Equations (3.4) and (4.2), the largest boulder required a storm wave 12.5 m high to move it. The equivalent tsunami wave was only 3.1 m

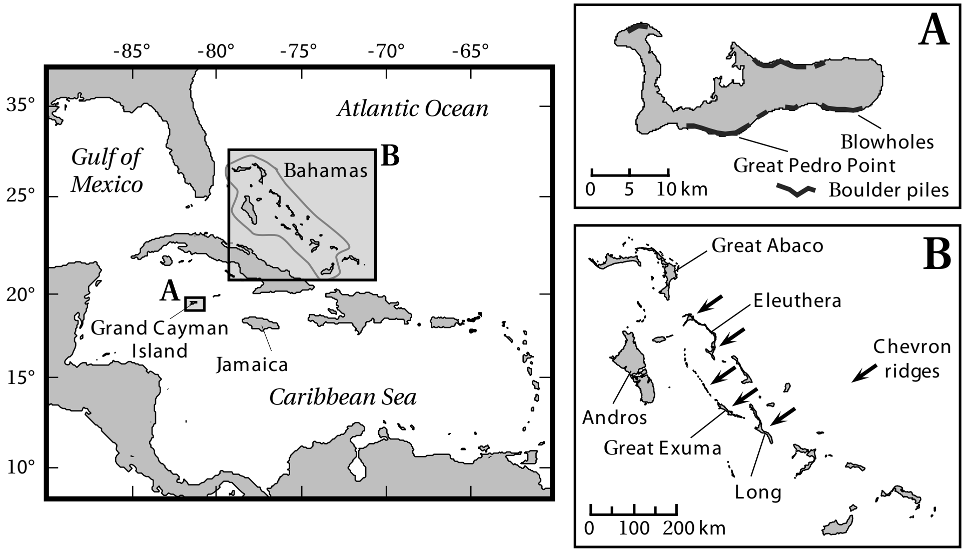

Figure 4.15. The Caribbean region. (A) Grand Cayman Island, and (B) the Bahamas.

high. The storm waves could only exist if water depths were more than 16 m deep at the base of cliffs, otherwise they would have broken. This condition occurs at only one of the locations where boulders are found. Even here, it is doubtful if storm waves could have maintained sufficient energy to transport boulders more than 100 m–150 m inland.

Bahamas

(Hearty, 1997; Hearty, Neumann, and Kaufman, 1998)

A second example comes from the Bahamas (Figure 4.15b), where the landscape has been created by either tsunami or storm waves. The Bahamas offer a range of features suggestive of tsunami from the Last Interglacial. Most interesting are V-shaped ridges up to several kilometers in length that have penetrated inland from the exposed Atlantic Ocean side of the islands. The ridges are asymmetrical, averaging 3 km in length, with some exceeding 10 km. They are 20 m–100 m wide and stand 8 m–25 m high, increasing in elevation toward their tip. Some ridges indicate that waves must have run up to elevations of 40 m above sea level at the time of deposition. There are up to 30 ridges, some tucked into each other. Nowhere does this involve more than four ridges. The ridges have a consistent orientation to the west–southwest that varies by no more than 10° along 300 km of coastline, despite a 60° swing in the orientation of the shelf edge. Internally, the ridges contain low-angle cross-beds, scour-and-fill pockets, pebble layers, and bubbly textures characteristic of rapid deposition found at the swash limit of accreting sandy beaches. The steepest dipping beds are found toward the landward margin of the ridges. Because of their

Table 4.3. Comparison of tsunami and storm-wave heights required to transport boulders in the Bahamas.

Location	*Length* (m)	*Boulder width* (m)	*Thick-ness* (m)	*Volume* (m^3)	*Weight* (t)	*Height of tsunami at shore* (m)	*Breaking storm-wave height* (m)
Paleo-boulders	13.0	11.5	6.5	972	1,846	5.9	23.7
	14.0	7.3	6.7	685	1,301	2.6	10.5
	9.3	6.0	4.0	223	424	2.8	11.3
	8.1	5.7	5.5	254	482	1.9	7.7
	7.2	5.7	5.0	205	390	2.1	8.2
Modern	7.8	4.7	2.5	92	174	2.7	10.9
	4.9	4.5	1.2	26	50	4.0	16.1
	3.8	2.5	2.0	19	36	1.0	4.0
	3.8	3.2	1.5	18	35	1.9	7.8
	6.4	2.7	0.5	9	16	3.9	15.7

Source: Based on Hearty (1997).

shape and the fact that smaller ones lie nestled within large forms, they have been termed chevron ridges. It was similarities to these ridges, found at Jervis Bay, New South Wales, that led to this term being used to identify one of the prominent signatures of large tsunami.

The chevron ridges on Eleuthera Island are associated with huge boulders up to 970 m^3 in size and weighing up to 1,850 tonnes (Table 4.3). These have been transported over the top of cliffs more than 20 m high. The boulders were emplaced at the end of the Last Interglacial sea level highstand. They were transported up to 500 m landward—a distance greater than present-day boulders have been transported. The modern boulders are much smaller, averaging 22 m^3 in volume and weighing less than 175 tonnes (Table 4.3). However, some of these modern boulders are anomalous and suggestive of recent tsunami. For example, some have been transported up to 200 m landward and more than 10 m above sea level.

Again, Equations (3.4) and (4.2) can be used to resolve the difference between the capacity of theoretical tsunami and storm waves to transport these boulders. Note that in these calculations a density of 1.9 $g\,cm^{-3}$ has been used for the coral boulders. The largest of the modern coral boulders requires a storm wave about 16 m in height to be transported, whereas the paleo-boulders require maximum storm waves of about 24 m in height. Both of these sizes are difficult to obtain close to shore without breaking even under storm surges of 7 m–8 m that can be generated here by tropical cyclones. Local storms also do not account for the formation and consistent alignment of the chevron ridges. Tropical cyclones have winds that rotate around an eye that rarely exceeds 100 km in diameter. For the ridges to be produced by a cyclone, the storm would have had to maintain consistently strong winds and moved parallel to the islands over a much longer distance than is observed at present. The echelon nature of some chevron ridges, tucked one inside the other, also requires more than one storm—which appears unlikely.

Tsunami with a distant origin appear more feasible. The paleo and modern boulders require maximum tsunami wave heights of only 6 m and 4 m, respectively. Waves, as small as 1.0 m–2.0 m in height, could have moved some of the boulders. Tsunami generated by submarine landslides or asteroid impact with the ocean produce up to four waves in their wave train. This could easily account for up to four chevron ridges nestled one within another—all with the same orientation. While the Bahamas are subject to submarine landslides along the shelf margin, a local source can be ruled out because waves would have radiated outward from this source and not been able to produce the consistent ridge alignment over such an extended distance. Either distant submarine landslides or an asteroid impact in the Atlantic Ocean accounts for the ridges and boulder deposits in the Bahamas. These possibilities will be discussed further in subsequent chapters.

Chilean coast

(Lockridge, 1985; Paskoff, 1991; Ortlieb *et al.*, 1995; Paskoff *et al.*, 1995)

Of the world's entire coastline, the west coast of South America is one of the most prone to recurrent large tsunami (Figure 4.16). In the 20th century, 23 tsunamigenic

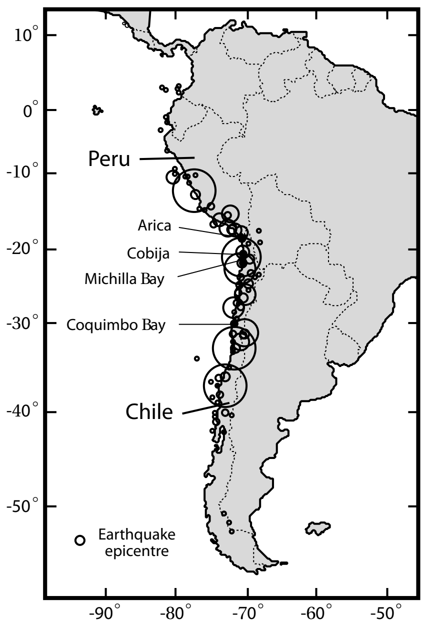

Figure 4.16. Location of historical tsunamigenic earthquakes since 1562 along the west coast of South America. Based on Intergovernmental Oceanographic Commission (1999). Size of circle is proportional to the number of events at the same site.

earthquakes have occurred along the coasts of Chile and Peru. Of these, 7 have had a surface wave magnitude, M_s, of 8.0 or more. Seismicity is linked to subduction of the Nazca Plate beneath the South American Plate. Earthquake epicenters tend to cluster along coastlines or at the base of the Andes Mountains (Figure 4.16). A narrow, uplifting coastal plain is constrained by the Andes Mountains, and subject to some of the largest tsunamigenic earthquakes in the world. The coastal plain is also old, recording the signature of past marine planations in the form of raised terraces that date back to the Miocene, more than 12 million years ago. Lower terraces have been reoccupied repetitively by Interglacial highstands in sea level during the past 2 million years.

Both the older terraces and the modern coastal plain preserve the signature of paleo-tsunami events. For example, at Herradurra Bay in the Coquimbo region, large tonalite boulders over 2 m in diameter are exposed within nearshore beach sands on a 200,000-year-old interglacial terrace that is now situated 35 m–40 m above sea level (Figure 4.17). The boulders originated 2 km away, on the Coquimbo Peninsula, which was an island at the time the terraces formed. The event that moved them was never repeated afterwards because boulders are not evident in younger deposits except where they have been eroded from the upper terrace. While boulders are uncommon in the present landscape, the signature of dump deposits is ubiquitous. One of the largest of these occurs at Michilla Bay in northern Chile. This dump

Figure 4.17. Boulders deposited by a catastrophic tsunami near Coquimbo Bay, 200,000 years ago. The boulders were transported more than 2 km and deposited in offshore waters. They have been tectonically uplifted since. Photograph courtesy Prof. Colin Murray-Wallace, School of Geosciences, University of Wollongong.

Figure 4.18. An elevated tsunami dump deposit at Michilla Bay, northern Chile. The event occurred around 7,100 years ago, coincidentally with sea level reaching its present level following the Holocene marine transgression. The ocean is to the right. The top of the terrace stands 6 m–7 m above sea level and about 1 km inland. Photograph courtesy Prof. Colin Murray-Wallace, School of Geosciences, University of Wollongong.

deposit is over 5 m thick, lies 7 m above present sea level, and consists of a massive bed of coarse sands interspersed with cobbles and large unbroken shells (Figure 4.18). Isolated boulders are scattered throughout the bottom of the deposit. Dating on the shell places the event about 7,000 years ago when sea level reached its present level following the Holocene marine transgression. Smaller Holocene events are also preserved as interstratified beds of pebbles and coarse sand within prehistoric middens, particularly in the Cobija area. In many respects, these deposits are similar to the disturbed Aboriginal middens of southeastern Australia described in the previous chapter.

Historically, tsunami have swept the total breadth of this plain and reached the base of the Andes. The most tsunamigenic section of coastline occurs on the border between Peru and Chile (Figure 4.16). Since historical records began in 1562, there have been 230 tsunami generated by earthquakes. Five localities have had ten or more tsunamigenic earthquakes over this period within a 110 km radius of each other. Three events have had Pacific-wide impact: the events of August 13, 1868 and May 10, 1877, both near the town of Arica on the present border between Peru and Chile, and the event of May 22, 1960. This latter event will be discussed in more detail in Chapter 5. The Arica events regionally had maximum run-ups of 21 m and 24 m,

Figure 4.19. The ruins of Cobija in northern Chile. The tsunami of May 10, 1877 destroyed the town, which was subsequently buried by alluvial gravels. The ruins contain layers of shelly sand brought ashore by the tsunami. Photograph courtesy Dr. Colin Murray-Wallace, School of Geosciences, University of Wollongong.

respectively, along the South American coast. Prior to these events, Arica had been destroyed twice by tsunami, in 1604 and 1705. The 1868 tsunami struck the town within half an hour of the main shock. The sea rose initially 5 m and then withdrew, leaving a 2 km wide strip of the seabed exposed. Several minutes later, the main wave came in and swept across the coastal plain (Figure 2.11).

Approximately 25,000 people lost their lives in this region alone. The tsunami then swept the Pacific Ocean, with damage being reported in New Zealand, Hawaii, and Japan. In Antarctica, the wave broke up sea ice. The 1877 event was just as large, if not more widespread. Its run-up was 20 m high at Arica and 24 m high at Tocopilla, 600 km south of the epicenter. The wave also swept the Pacific Ocean and had a particularly forceful impact on the coast of New Zealand, where run-up of 6 m was reported. In eastern Australia, the wave was responsible for the largest tsunami, 1.07 m, recorded on the Sydney tide gauge. These historical tsunami have repetitively destroyed coastal towns and moved layers of coarse sand shoreward. For example, Figure 4.19 shows the ruins of Cobija in northern Chile, wiped out by the Arica tsunami of May 10, 1877. The wave arrived 5 minutes after the earthquake and reached 11.9 m above mean sea level at this location, eroding into raised alluvial fans, which can be seen in the background. Backwash buried the ruins in gravels interspersed by layers of shelly sand brought ashore by the tsunami. Despite this precarious environment, rebuilding has always taken place even at the most vulnerable sites. Today, in many places, evacuation from tsunami would be difficult even with adequate warning because sea cliffs back numerous towns.

Storms are significant events in the coastal environment. Nonetheless, tsunami are an alternative mechanism for reworking coastal sediment and ultimately for imprinting upon the landscape a signature of convulsive events that in some areas has not been removed over thousands of years. The difficulty in invoking storms for all coastal deposition and erosion lies not just in the insufficient magnitude of observed events but also in the inapplicability of storm wave processes to account for a suite of anomalous deposits. For instance, dump deposits, bouldery mounds, and chevron ridges contain chaotic mixtures of sediment that cannot be explained by storm waves because such waves erode sand from the shoreline, transport coarse sediment shoreward as a body, and sort debris in a shore normal direction. Storms also cannot account for bedrock sculpturing. Tsunami can move and deposit highly bimodal sediment mixtures and create the suites of high-magnitude depositional and erosional signatures that dominate many landscapes worldwide. This evidence cannot be ignored. The only question that remains is, "What causes these tsunami?" To answer this question one must examine the type of deposits and landscapes produced by earthquakes, volcanoes, and submarine landslides that are the main causative mechanisms of tsunami. In addition, asteroid impacts with the ocean cannot be ignored despite having never occurred historically. As will be shown, the flux of comets and asteroids has been substantially greater over the past two millennia than at present. This increased frequency has been observed and reported in legends, but never in documents that can be interpreted from a modern perspective, or that can withstand the scrutiny of contemporary scientific methodology. Authentication of asteroid-generated tsunami as an underrated and significant hazard will be presented in Chapter 8.